J Nanostruct 16(2): 2050-2059, Spring 2026

RESEARCH PAPER

Influences of Incorporating $AgNO_3$-$BaTiO_3$ NPs on the Microstructure and Electrical Properties of PVA/PEO Polymers Matrix

Zahraa A. Nayyef *, Abdulazeez O. Mousa Al-Ogaili, Ameerah A. Al-Sadooni

Department of Physics, College of Science, University of Babylon, Babylon 51001, Iraq

ARTICLE INFO

Article History:
Received 05 December 2025
Accepted 17 March 2026
Published 01 April 2026

Keywords:
$AgNO_3$-$BaTiO_3$ NPs
Electrical Properties
Surface materials
XRD

ABSTRACT

The present study included the investigate the influence of incorporating (silver nitrate $AgNO_3$) and (barium titanate $BaTiO_3$) into (polyvinyl alcohol PVA)/(polyethylene oxide PEO) matrix. These materials was fabricated using casting method. Enhance the microstructure and electrical characteristics of polymer matrix by adding nanoparticles is an effective technique for developing advanced functional materials. The X-ray diffraction (XRD) measured confirmed the semicrystalline structure of polymer. The strongest peak appeared at $2\theta = 31.57°$. Other strong diffraction peak were observed at $2\theta = 19.58°$ and 19.5°. The crystallinity increased after adding the nanoparticles at $2\theta = 22.1°$, 23.59°, and others. Field-emission scanning electron microscope (FESEM) the images showed that adding nanoparticles improved the surface structure. Energy-dispersive X-ray spectroscopy (EDS) results showed that the pure PVA/PEO blend mainly contained carbon and oxygen, after incorporating nanoparticles, additional elements such as Ti, Ag, and Ba. Electrical measurements showed that the dielectric constant and dielectric loss were high at low frequencies. It was also observed that adding of nanoparticles increased the polarizability and electrical conductivity of the samples.

How to cite this article
Nayyef Z., Al-Ogaili A., Al-Sadooni A. Influences of Incorporating $AgNO_3$-$BaTiO_3$ NPs on the Microstructure and Electrical Properties of PVA/PEO Polymers Matrix. J Nanostruct, 2026; 16(2):2050-2059. DOI: 10.22052/JNS.2026.02.051

INTRODUCTION

The (PVA/PEO) polymers are prominent materials in various medical, industrial, and electronic applications, because their unique properties including thermal stability, water solubility, and ease of shaping and processing [1]. Recent years have seen growing interest in enhancing polymer properties through the introduction of nanomaterials such as ($AgNO_3$) ($BaTiO_3$), given their ability to improve polymers' mechanical, thermal, and functional characteristics. These nanomaterials enhance structural stability, increase strength and durability, and improve electrical or thermal conductivity, thereby expanding the range of industrial, medical, and electronic applications for conventional polymers [2]. The (PVA) polymer prepared from the polymerization of vinyl acetate followed by alcoholysis. It has been widely used as films [3,4]. (PEO) is a hydrophilic, nonionic, water-soluble polymer that is used to deliver scaffold fabrication, drugs, and tissue engineering [5]. Polymers, blends, and composites have many novel properties, including: low cost,

---

* *Corresponding Author Email: sci618.zahraa.ali@uobabylon.edu.iq*

flexibility and high resistance, that make them particularly useful in various applications of electronic technique. Currently polymer science is a cutting-edge field due to the high strength, excellent corrosion resistance, and good thermal stability of polymers [6]. These materials are also characterized by their low cost, ease of processing, mechanical strength, and flexibility. Because of these properties, polymers have become essential components in many industrial applications, including microelectronics and photolithography. Composite materials have also emerged as important modern engineering materials due to their unique properties such as light weight and ease of assembly. These materials are widely used in electronic packaging for medical equipment, in aircraft manufacturing, and in the production of low-cost, lightweight polymer composites [7]. Currently composite materials refer to materials reinforcement surrounded by a weaker matrix material. The matrix serves to distribute the reinforcement and also to transmit the load to the reinforcement [8]. Composite nanomaterials are of great importance due to their unique physical and chemical properties. The interactions and fine dispersion of these particles within the polymer are key factors in developing the properties of these materials, such as their microstructure and electrical characteristics. [9,10]. In this research, the addition of nanoparticles to the polymers matrix increased the state of crystallinity. The A.c measurements showed that the dielectric constant and dielectric loss values are high at low frequencies consistent with previous studies Ref [11]. The main objective of this research is to analyze the effect of nano-particles on the microstructure and electrical characteristic of polymers blend to make them suitable for many use for example sensors, batteries, and active membranes.

MATERIALS AND METHODS

The materials used in this study were classified into two main categories: polymers and nanomaterials. The polymer components included polyvinyl alcohol (PVA) with a molecular weight of 14,000 g/mol, produced by BDH Chemicals Ltd (England), and polyethylene oxide (PEO) with a molecular weight of 3×10^6 g/mol, produced by Cheng Du Micxy Chemical Co., Ltd. Both polymers are white, water-soluble, organic powders. The nanomaterials consisted of silver nitrate ($AgNO_3$) with a molecular weight of 169.87 g/mol, produced by a company in California, USA, and barium titanate ($BaTiO_3$) with a molecular weight of 233.19 g/mol, produced by Research Nanomaterials, Inc., Houston, Texas, USA. Silver nitrate is a transparent, water-soluble inorganic compound, while barium titanate is a white, water-soluble inorganic substance.

Preparation of nanocomposite films

The sample (Ao, A1 and A2) was prepared by casting method with different weights as listed in Table 1. The step two was to dissolve the specified weights of polymers in DI water (H_2O) using a magnetic stirrer at room temperature (21 °C) for (2 h) to obtain good solution. The solution was cast into a 6 cm Petri dish and dried (12) days in a dust-free environment.

Instruments used

The X-ray device using (Aeris-Malvern Panalytical) I = 7.5 kv, **λ=** 1.54 Å. FESEM analysis of the samples were measured using (Inspect F50-FEI company), 30.00 kV high voltage, and EDS measured using (Axia ChemiSEM- Thermo Scientific company) acceleration voltage 30 kV. AC

Table 1. The weight percentages of each sample.

Sample	PVA	PEO	$AgNO_3$	$BaTiO_3$
Ao	0.80	0.20	0	0
A1	0.80	0.140	0.015	0.045
A2	0.80	0.125	0.015	0.060

analysis of the samples were measured using (LCR Meter).

RESULTS AND DISCUSSION

XRD analysis

In Fig. 1 showed the XRD results of pure (PVA/PEO) blend and the nanocomposite films of (PVA, PEO, AgNO3 and BaTiO3). The result of pure polymers shows semicrystalline nature, with high peaks at 2θ = 22.1°, 19.58°, and 23.59° these peaks correspond to the (133), (040) and (133) crystal structures of (PVA/PEO) blend as shown in Fig. 1a. The semicrystalline nature of these polymers plays a fundamental role in ensuring both chemical and electrochemical stability. Crystallization in polymeric systems generally proceeds through a hierarchical organization that spans multiple structural scales. Throughout this process, polymer chains undergo folding, leading to the formation of distinct lamellar structures characterized by specific molecular arrangements. This folded-chain configuration allows lateral growth in two dimensions while restricting chain propagation in the perpendicular direction, where structural imperfections are predominantly localized at the fold surfaces. While previous work [12] investigated the structural features of the pristine PVA/PEO blend withe spacific wights of nanoparticels, but the present study usded the same pure sample (Ao) to compare, extends this analysis by examining the influence of modified weight ratios and the emergence of additional crystalline phases, the resule consistent with those reported in previous studies [13]. However, this research presents a more comprehensive structural analysis, revealing improved ordering and the emergence of additional crystalline phases using new sample weight ratios. Fig. 1b, showed three high peaks at (2θ = 22.4°, 19.48°, and 23.59°) observed correspond to the (133), (040), and (133) crystal structures of polymers. And other peaks were also showed as a result of adding nanomaterials. peak at (2θ = 31.82° and 39.77°) correspond to the (200) and (220) crystal structures of $AgNO_3$, the Braggs angle of ($AgNO_3$) agrees with JCPDS data (Code 96-210-5349), peak at (2θ = 31.82°, 45.48° and 56.42°) correspond to the (110), (200) and (211) crystal structures of $BaTiO_3$, the Braggs angle of ($BaTiO_3$) agrees with JCPDS data (Code 96-152-5438).

Fig. 1c shows peaks at (2θ = 22.17°, 19.5° and 23.35°) observed correspond to the (220), (131) and (025) crystal structures of PVA/PEO. Peaks at (2θ = 31.57° and 39.69°) correspond to the (200)

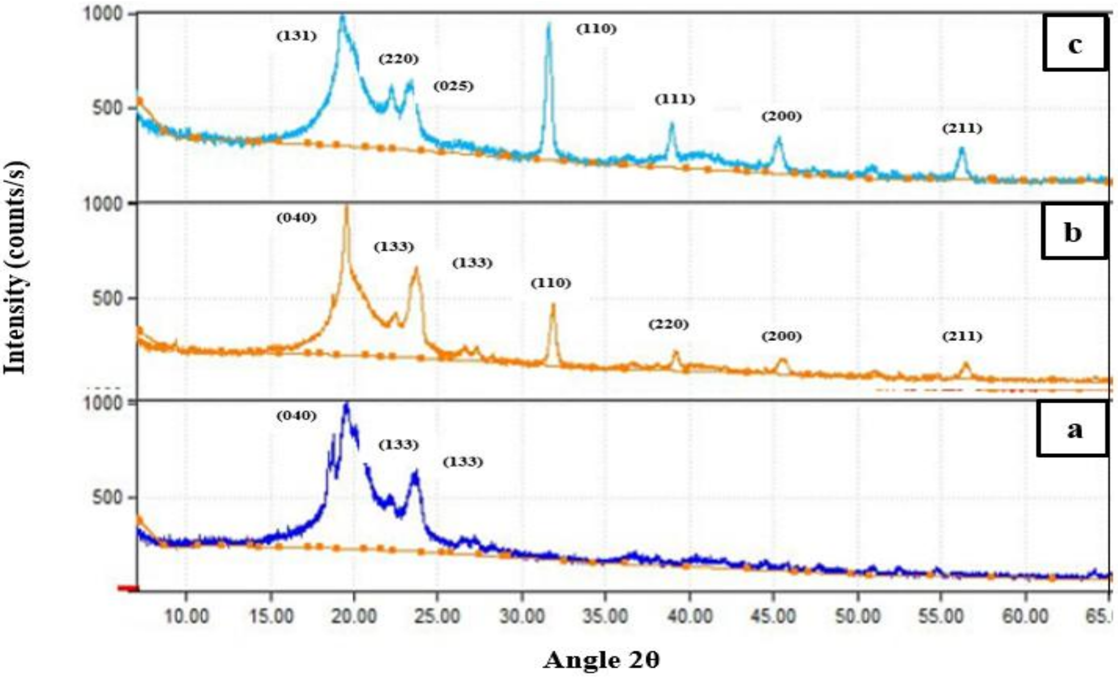

Fig. 1. Result of XRD (a) of polymer blend (Ao), (b) and (c) polymer blend with nanoparticles films of (A1) and (A2).

and (220) crystal structures of $AgNO_3$, and peaks at (2θ = 22.17°, 31.57°, 39.69°, 45.23°, and 56.17°) correspond to the (100), (110), (111), (200), and (211) crystal structures of $BaTiO_3$. Although some of the results are consistent with those reported in previous studies [14, 15] regarding the general behavior of the polymer, this study stands out for its novel scientific contribution in revealing the formation of additional crystalline phases not recorded in those studies, indicating a stronger interaction between the PVA/PEO mixture and the $AgNO_3$ and $BaTiO_3$ nanoparticles. In summary, the results of XRD show that more nanoparticles adding to the polymers blend leads to an increase in peaks. This is due to structural changes in the polymer matrix, which may result in alterations in the degree of polymer crystallinity and shifts in the arrangement of polymer chains. Several coefficients can be derived from the X-ray diffraction peaks, where the distance between crystalline planes (d) is calculated by Brag equation (1) [16]:

$$n\,\lambda = 2d\sin(\theta) \tag{1}$$

Where n, λ, and (θ) mean the integer, wavelength, and angle of the X-ray respectively. The crystal size (D) is calculated by using Debye-Scherer formula (2) [17]:

$$D = k\lambda \,/\, \beta\cos(\theta) \tag{2}$$

k = 0.9 is the crystals factor, and (β) is full width at half the maximum of peak (FWHM), as shown in Table 2. The strain of lattice (Ɛ) is calculated by applied equation (3) [17]:

$$\varepsilon = \beta \,/4\tan(\theta) \tag{3}$$

The size of crystal (D) was impacted and increased when add the ($AgNO_3$ and $BaTiO_3$) in matrix of polymer. Table 2 show important parameters of XRD measurements.

Field-emission Scanning Electron Microscope (FESEM)

Field-emission Scanning Electron Microscope (FESEM) is a type of high-resolution microscope used to visualize very small topographic details on the surface or entire or fractioned objects [18]. FESEM is widely used in nanotechnology, and science of materials etc. where surface analysis and excellent of resolution are important [19]. The morphologies of the films were rigorously surveyed, examined, and studied in Fig. 2.

The FESEM result of the pure polymers blend shows the morphology is smoother surface within some is rough surface and largely homogeneous due to its semicrystalline structure of polymers,

Table 2. X-ray parameters of films.

Sample		2θ (deg)	Int. (c/s)	(hkl)	d (Å)	β (deg)	Crystal size (Å)	Strain of lattice
A_O	PVA	22.1	1295.97	(133)	3.998	1.008	45	4.43
	PEO	19.58	2543.89	(040)	4.530	1.454	31	7.27
		23.59	1489	(133)	3.768	0.877	74	2.55
A1	PVA	22.4	1128.73	(133)	3.964	0.888	75	2.65
	PEO	19.48	2614.51	(040)	4.552	0.403	136	1.67
		23.59	1703.18	(133)	3.793	0.6618	133	1.42
	$AgNO_3$	31.82	1250.75	(200)	2.809	0.387	225	0.62
		39.77	400.99	(220)	2.264	4.235	11	9.98
	$BaTiO_3$	31.82	1250.75	(110)	2.809	0.387	225	0.62
		45.48	492.87	(200)	1.992	0.618	109	0.91
		56.42	422.93	(211)	1.629	0.465	177	0.46
A2	PVA	22.17	1061.06	(220)	4.005	1.011	45	4.45
	PEO	19.5	1553.85	(131)	4.547	1.795	34	6.76
		23.35	1108.12	(025)	3.806	0.963	54	3.52
	$AgNO_3$	31.57	1656.66	(200)	2.831	0.380	223	0.63
		39.69	425.58	(220)	2.269	4.873	11	10.56
	$BaTiO_3$	22.17	1061.06	(100)	4.005	1.011	45	4.45
		31.57	1656.66	(110)	2.831	0.380	223	0.63
		39.69	425.58	(111)	2.269	4.873	11	10.56
		45.23	571.71	(200)	2.003	0.523	126	0.79
		56.17	510.64	(211)	1.636	0.481	2.3	0.4

as for the size particle (56.85 - 94.58) nm, as shown in Fig. 2a. $AgNO_3$ and $BaTiO_3$ The addition of nanoparticles contributed significantly to modifying the properties of the polymer matrix,

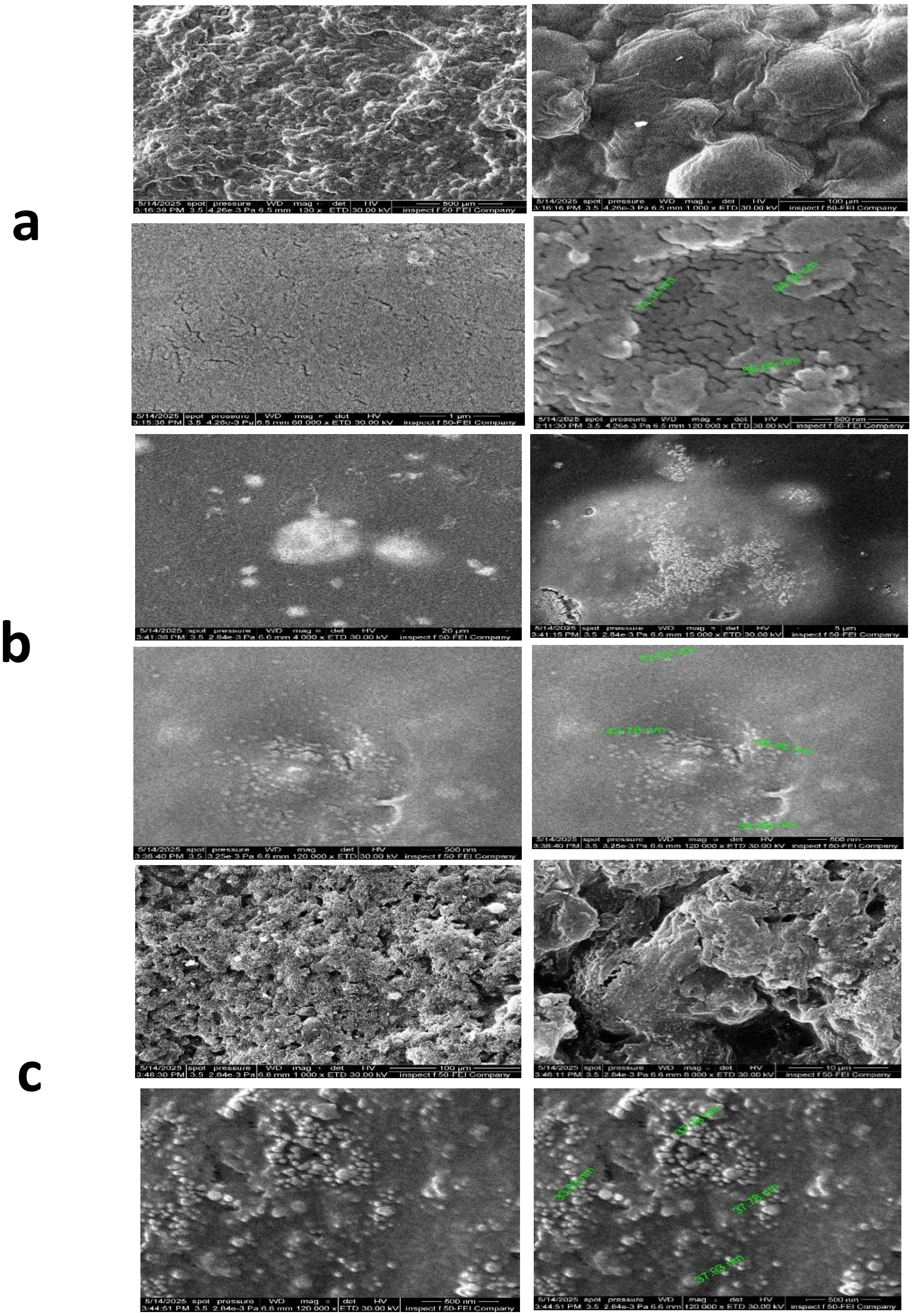

Fig. 2. FESEM analysis of nanocomposite films: (a Ao (b) A1 (c) A2.

which was characterized by uniform dispersion and granular structure without the appearance of obvious clumps. These particles appear spherical or sub-spherical and the particle size ranges

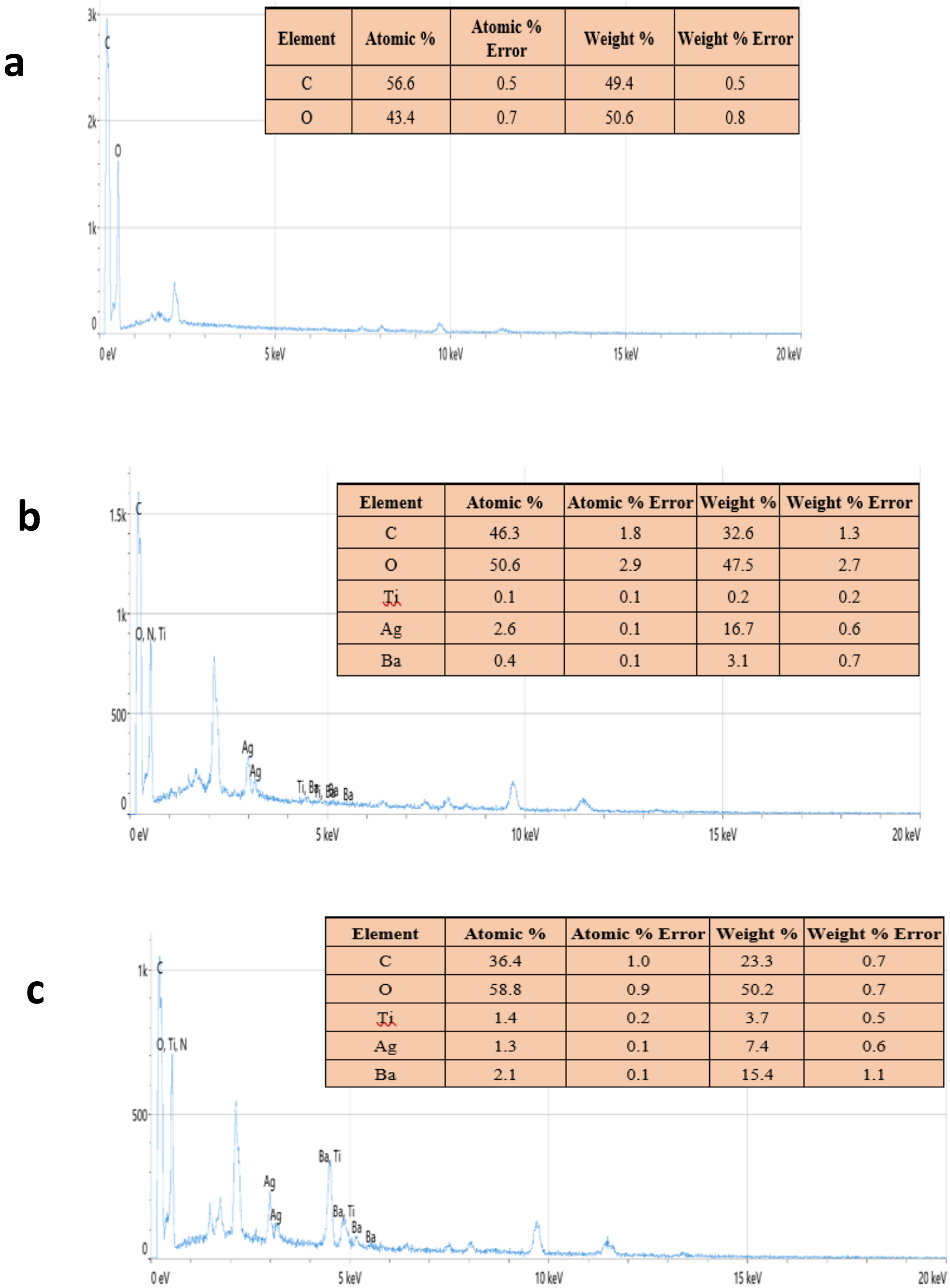

a

Element	Atomic %	Atomic % Error	Weight %	Weight % Error
C	56.6	0.5	49.4	0.5
O	43.4	0.7	50.6	0.8

b

Element	Atomic %	Atomic % Error	Weight %	Weight % Error
C	46.3	1.8	32.6	1.3
O	50.6	2.9	47.5	2.7
Ti	0.1	0.1	0.2	0.2
Ag	2.6	0.1	16.7	0.6
Ba	0.4	0.1	3.1	0.7

c

Element	Atomic %	Atomic % Error	Weight %	Weight % Error
C	36.4	1.0	23.3	0.7
O	58.8	0.9	50.2	0.7
Ti	1.4	0.2	3.7	0.5
Ag	1.3	0.1	7.4	0.6
Ba	2.1	0.1	15.4	1.1

Fig. 3. EDS analysis of. (a) PVA/PEO polymer blend film of Ao (b) A1 (c) A2.

between (33.03 - 43.78) nm as shown in Fig. 2b.

The increasing of loading of ($AgNO_3$ and $BaTiO_3$) revealed formalizing spherical shapes, the porous structure of the sample (A2) indicates its potential for applications requiring high surface area, such as sensors or electrochemical materials. Given that barium titanate ($BaTiO_3$) exhibits insulating properties, this enhances the sample's potential for the fabrication of ionic conduction films or capacitors, The particles size range between (33.03 - 37.93) nm. The surface is more compact and the particle structure is clear as shown in Fig. 2c, The results indicate that $AgNO_3$ and $BaTiO_3$ particles are uniformly distributed within the polymers matrix, which can be explained by the compatibility between the polymer components and its ability to effectively contain the composite nanoparticles [20].

Energy Dispersive X-ray Spectrometry (EDS)

The (EDS) is used to analyze withe detect components to determine the chemical properties of films. Both oxygen and carbon appear as representatives of blend polymer [13]. The composition of elemental of polymer blend for (Ao) Fig. 3a showed the amounts of Carbon and Oxygen elements at 56.6% and 43.4% resistively. The EDS of polymers with nanoparticles films for (A1) Fig. 3b showed the C, N, O,Ti, Ag and Ba elements at the amounts of (46.3, 50.6, 0.1, 2.6, and 0.4) wt.%, respectively. EDS of PVA/PEO, $AgNO_3$ and $BaTiO_3$ films for (A2) Fig. 3c verified the existence of C, O, Ti, Ag and Ba elements at the amounts of (36.4, 58.8, 1.4, 1.3, and 2.1) wt.%, respectively. The data indicate that the high-intensity element is oxygen, which can be attributed to the polymer composition.

Electrical Properties (AC)

Dielectric constant and loss factors are the most convenient and efficient methods to investigate the structure of polymers. The electrical conductivity of insulating polymer can enhance by additive nanoparticles. Dielectric constant (έ) the ratio between the capacitance of a capacitor filled with a dielectric medium and that of the same capacitor when the region between its plates is a vacuum [21, 22].

$$\acute{\varepsilon} = Cp/Co \tag{4}$$

Where: Cp and Co are vacuum capacitance parallel.

Figs. 4 and 5 shows that the dielectric constant and dielectric loss with variations frequency (f) that both have good-values at lower frequency, due to the nature that dipole moments have ample time in these zones to order themselves in the direction of the applied electric field. The dielectric constant and dielectric loss decrease monotonically and reach constant value as the frequency increases.

The dielectric loss (ε″) determine by [23]:

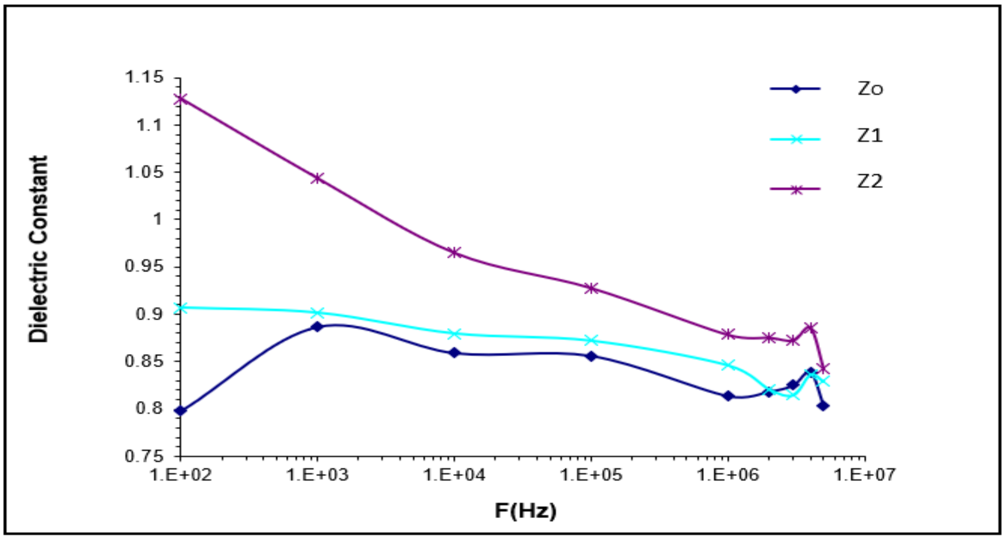

Fig. 4. Dielectric constant versus frequency f of PVA, PEO, $AgNO_3$ and $BaTiO_3$ films.

$$\varepsilon'' = \acute{\varepsilon}\, D \quad (5)$$

Where: D is coefficient of dispersion of nanoparticles.

With increasing frequency, the dielectric constant changes, the polarization of the space charge decreases, as a greater number of ions cannot diffuse in the direction of the applied electrical field, because the dielectric characteristics are low affected by charge carriers [22]. With increasing nanoparticles, the dielectric constant and loss decrease as a result of increased electrical conductivity due to increased charge carriers. [23, 24].

In Fig. 4 all samples (A_O, A1 and A2) show a slight decrease in dielectric constant with increasing frequency. A2 has the highest dielectric constant value at low frequencies. Ao has approximately the lowest value. At low frequencies, the various

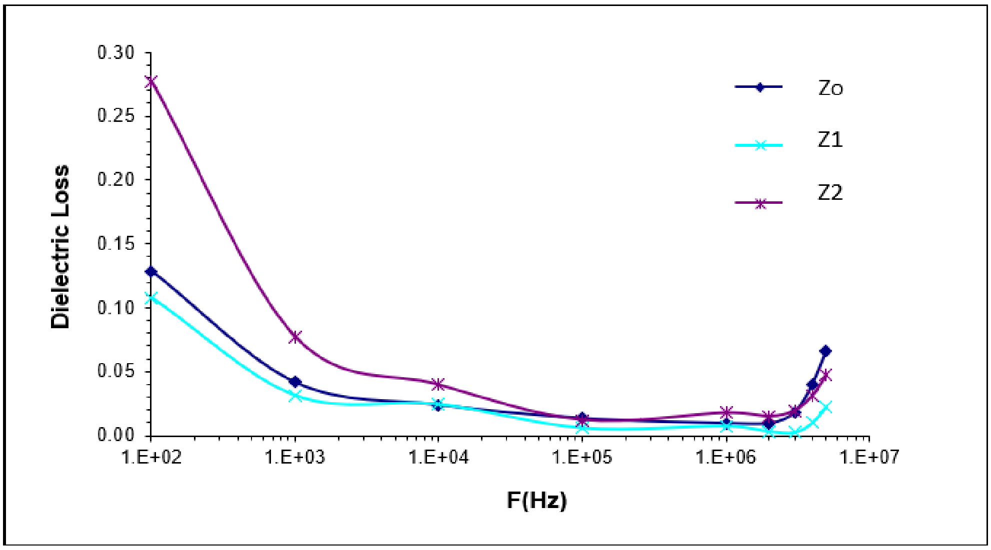

Fig. 5. Dielectric loss versus frequency f of PVA, PEO, $AgNO_3$ and $BaTiO_3$ films.

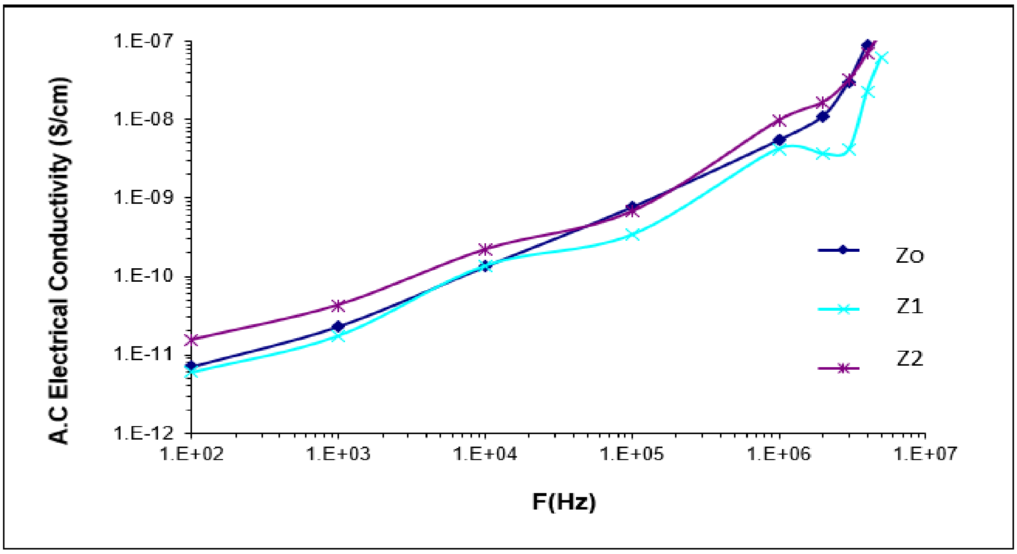

Fig. 6.AC electrical conductivity versus frequency f of PVA, PEO, $AgNO_3$ and $BaTiO_3$ films.

polarizations (ionic, dipole, and intergranular) contribute significantly, resulting in a high dielectric constant value. By adding $AgNO_3$ and $BaTiO_3$ in (A1, A2), the sample's polarizability increases, especially with A2 (which may have the highest concentration). At high frequencies, the polarizability decreases due to delayed charge movement, so the dielectric constant decreases.

Fig. 6 illustrates the variation of electrical conductivity as a function of frequency. The observed behavior can be attributed to interfacial polarization effects associated with A.C. conductivity, which progressively increases with increasing frequency. Furthermore, an enhancement in electrical conductivity was recorded with rising nanoparticle (NPs) content, likely due to the increased charge carrier density within the polymer blend matrix [24]. All samples show an increase in conductivity with frequency. A2 exhibit the highest conductivity values at most frequencies. Samples containing $AgNO_3$ and $BaTiO_3$ show improved conductivity due to the ionic conductivity of the silver nitrate and the high dielectric properties of barium titanate, which improves the polarization of the medium and the release of charges. Best performance in terms of conductivity and dielectric constant (A2). Best performance in terms of stability low loss A1.

The electrical conductivity was determine by [25]:

$$\sigma A.C = \omega\, \varepsilon''\, \varepsilon_o \qquad (6)$$

CONCLUSION

The finding of the work showed that the adding of nanoparticles into matrix of polymers due to develop the crystallinity. XRD measurement observed the higher peak at 2θ = 31.57° due to crystal planes of the $BaTiO_3$ lattice. New peaks showed at 2θ = 31.82°, 39.69°, 45.23° and 56.17° when nanoparticles was adding due to increasing crystallinity. Correspond (133), (040), (133), (110), (111), (200) and (211) crystal planes and others. Decrease in lattice strain were observed after adding nanoparticles to the polymer matrix. This is attributed to the improved crystallization process. The FESEM results confirm that the $AgNO_3$ and $BaTiO_3$ nanoparticles were uniformly distributed within the PVA/PEO matrix without obvious agglomerations, contributing to improved surface uniformity and density. The porous structure of sample (A2) and the fine particle size ranging from (33.03 - 94.58) nm support the potential use of these films in nanodevice applications, such as sensors, ionic conduction films, and high-performance capacitors. EDS analysis showed a clear improvement in the composition of elemental of the polymer blend films after the addition of $AgNO_3$ and $BaTiO_3$ nanoparticles. The carbon content gradually decreased from 56.6% to 36.4%, and the oxygen content increased from 43.4% to 58.8%, indicating an increase in the oxide content in the surface structure. The presence of Ti, Ag, and Ba elements at concentrations ranging from (0.1–2.6) % also confirmed the effective homogeneity of particle distribution within the polymer matrix. These results support the success of the nano loading process and the improvement of the structural properties of the films. The results of electrical properties indicate of the PVA/PEO films were affected by the presence of nanoparticles. Their incorporation increased the medium's polarization and improved charge mobility, reflected in the higher conductivity and dielectric constant of sample A2 compared to the pure sample. The insulating properties of barium titanate and the ionic conductivity of silver nitrate also contribute to improved overall electrical performance and reduced dielectric loss, making these films promising for highly efficient sensor and electrochemical device applications.

ACKNOWLEDGMENT

The authors gratefully acknowledge the support and guidance provided by the Department of Physics, College of Science, University of Babylon. They also thank Dr. K. Abdali and Dr. Huda Raad for their helpful contributions.

CONFLICT OF INTEREST

The authors declare that there is no conflict of interests regarding the publication of this manuscript.

REFERENCES

1. Al-jamal AN, Hadi QM, Hamood FJ, Abass KH. Particle Size Effect of Sn on Structure and Optical Properties of PVA-PEG Blend. 2019 12th International Conference on Developments in eSystems Engineering (DeSE); 2019/10: IEEE; 2019. p. 736-740.
2. Sharba KS. Enhancement of Urbach Energy and Dispersion Parameters of Polyvinyl Alcohol with Kaolin Additive. Neuroquantology. 2020;18(3):66-73.
3. Gohil JM, Bhattacharya A, Ray P. Studies on the Crosslinking of Poly (Vinyl Alcohol). Journal of Polymer Research. 2005;13(2):161-169.

4. Mansur HS, Sadahira CM, Souza AN, Mansur AAP. FTIR spectroscopy characterization of poly (vinyl alcohol) hydrogel with different hydrolysis degree and chemically crosslinked with glutaraldehyde. Materials Science and Engineering: C. 2008;28(4):539-548.
5. Bromberg L. Poly(ethylene oxide)-b- Poly(propylene oxide)-b-Poly(ethylene oxide)-g-Poly(acrylic acid) Copolymers as In Situ Gelling Vehicle for Nasal Delivery. Drugs and the Pharmaceutical Sciences: Informa Healthcare; 2002. p. 749-758.
6. Rasheed MH, Hashim FS, Abass K. Impact of Fe2o3 Nanoparticles on the Spectral and Optical Properties of Electrospun Nanofibrous Poly Vinyl Alcohol/ Poly Acrylamide. Elsevier BV; 2023.
7. Study of Optical Properties for (PVA-PEG-ZnO) Nanocomposites. International Journal of Science and Research (IJSR). 2016;5(5):1794-1799.
8. Composite Materials for Other Applications. Composite Materials: CRC Press; 2002. http://dx.doi.org/10.1201/9781420031683.ch8
9. Firdaus RM, Rosli NIM, Ghanbaja J, Vigolo B, Mohamed AR. Enhanced adsorption of methylene blue on chemically modified graphene nanoplatelets thanks to favorable interactions. J Nanopart Res. 2019;21(12).
10. Hussein S. A Study of Some Mechanical and Physical Properties for Palm Fiber/Polyester Composite. Engineering and Technology Journal. 2020;38(3B):104-114.
11. Al-Bermany E, Mekhalif ATm, Banimuslem HA, Abdali K, Sabri MM. Effect of green synthesis bimetallic Ag@SiO2 core–shell nanoparticles on absorption behavior and electrical properties of PVA-PEO nanocomposites for optoelectronic applications. Silicon. 2023;15(9):4095-4107.
12. Nayyef ZA, Al-Ogaili AOM, Al-Sadooni AA. Effect of Decoration $AgNO_3$ - $BaTiO_3$ Nanoparticles on the Structure and Optical Properties of PVA/PEO Polymer Blend. Revue des composites et des matériaux avancés. 2025;35(06):1211-1216.
13. Hassan AAM, Al-Ogaili AOM. The Impact of Psyllium Husk Addition on the Some Physical Properties of PEO Polymer. Revue des composites et des matériaux avancés. 2025;35(1):71-79.
14. Saini I, Rozra J, Chandak N, Aggarwal S, Sharma PK, Sharma A. Tailoring of electrical, optical and structural properties of PVA by addition of Ag nanoparticles. Materials Chemistry and Physics. 2013;139(2-3):802-810.
15. Beena P, Jayanna HS. Dielectric studies and AC conductivity of piezoelectric barium titanate ceramic polymer composites. Polym Polym Compos. 2019;27(9):619-625.
16. Yang Z, Zhang Y, Wen B. Enhanced electromagnetic interference shielding capability in bamboo fiber@polyaniline composites through microwave reflection cavity design. Composites Science and Technology. 2019;178:41-49.
17. Qiu M, Zhang Y, Wen B. Facile synthesis of polyaniline nanostructures with effective electromagnetic interference shielding performance. Journal of Materials Science: Materials in Electronics. 2018;29(12):10437-10444.
18. Goldstein JI, Newbury DE, Echlin P, Joy DC, Lyman CE, Lifshin E, et al. Special Topics in Scanning Electron Microscopy. Scanning Electron Microscopy and X-ray Microanalysis: Springer US; 2003. p. 195-270.
19. Di Marco G. Solid state electrochromic device: behaviour of different salts on its performance. Solid State Ionics. 2000;127(1-2):23-29.
20. Jaramillo LY, Vásquez-Rendón M, Upegui S, Posada JC, Romero-Sáez M. Polyethylene-coffee husk eco-composites for production of value-added consumer products. Sustainable Environment Research. 2021;31(1).
21. Federico PJ. [Patent Office correspondence, 1814-1836: s.n; 1988.
22. Leighton PA. Electronic Processes in Ionic Crystals (Mott, N. F.; Gurney, R. W.). J Chem Educ. 1941;18(5):249.
23. Ngai KS, Ramesh S, Ramesh K, Juan JC. A review of polymer electrolytes: fundamental, approaches and applications. Ionics. 2016;22(8):1259-1279.
24. Itoh T. Composite polymer electrolytes based on poly(ethylene oxide), hyperbranched polymer, BaTiO3 and LiN(CF3SO2)2. Solid State Ionics. 2003;156(3-4):393-399.
25. Praveenkumar K, Sankarappa T, Ashwajeet JS, Ramanna R. Dielectric and AC Conductivity Studies in PPy-Ag Nanocomposites. Journal of Polymers. 2015;2015:1-5.